Visualizing invisible dark matter annihilation with the CMB and matter power spectrum

Yanou Cui and Ran Huo

Visualizing Invisible Dark Matter Annihilation with the CMB and Matter Power Spectrum

Yanou Cui[1, *] and Ran Huo[1, †]

[1]*Department of Physics and Astronomy, University of California, Riverside, California 92521, USA*
(Dated: May 17, 2019)

We study the cosmological signatures of Invisibly Annihilating Dark Matter (IAnDM) where DM annihilates into dark radiation particles that are decoupled from the Standard Model (SM). In the simple benchmark model we consider here such invisible annihilation determines the relic abundance of DM via dark thermal freezeout. We demonstrate that IAnDM may reveal itself through observable, novel signatures that are correlated: scale-dependent $\Delta N_{\rm eff}$ (number of extra effective neutrinos) in the Cosmic Microwave Background (CMB) spectrum due to DM residual annihilation, while the phase of acoustic peaks shift towards the opposite direction relative to that due to SM neutrinos, resembling the effect due to scattering (fluid-like) thermal dark radiation; in addition, IAnDM induces modifications to the matter power spectrum that resemble that due to warm dark matter. Current data is sensitive to IAnDM with masses up to ~ 200 keV, while future observations will improve the reach, especially if the late-time DM annihilation cross-section is enhanced relative to the standard thermal value, which can be realized in a variety of scenarios. This work also demonstrates a new possibility of realizing thermal sub-MeV DM with observable signals.

I. Introduction

Over the past two decades, we have seen overwhelming gravitational evidence for the existence of dark matter (DM) which constitutes 80% of the total matter density in our universe today. Nevertheless, the non-gravitational, particle nature of DM remains mysterious. Among the many theoretical candidates for DM, the Weakly Interacting Massive Particle (WIMP) is a well-motivated scenario that has played a central role in guiding the experimental searches for DM. The key process in WIMP models is the annihilation of DM into Standard Model (SM) particles which determines the relic abundance of DM after its thermal freezeout in the early universe. The residual DM annihilation today is potentially observable through indirect detection experiments, and via the Cosmic Microwave Background (CMB) observations which is free of astrophysical uncertainties [1–3]. These CMB studies focus on the effects of *visible* SM states (e.g., $e^{\pm}, \gamma$) on the recombination history of the universe.

Recently, driven by the strengthening experimental constraints on WIMP DM, there has been a growing interest in dark sector scenarios, where DM resides in a hidden sector with multiple states and/or self-interactions, in analogy to the complex structure of the SM. In simple benchmark model that we focus on here the merit of predicting DM relic abundance from thermal freezeout is retained, yet the DM predominantly annihilates into other dark states instead of SM particles [4–16]. By decoupling the thermal relic abundance from couplings to the SM, these models are relieved from conventional DM constraints, yet call for new strategies for detection. The most challenging case arises when DM undergoes *invisible annihilation*, i.e., when DM annihilates into stable dark radiation (DR) particles that are decoupled from the SM. Can we *directly* observe/constrain this apparent nightmare (yet minimal and generic) scenario of Invisibly Annihilating DM (IAnDM) with cosmological data? In this paper we will demonstrate a positive answer to this question: while the thermal $\Delta N_{\rm eff}$ of DR [13] in IAnDM can be significantly suppressed if the dark sector is much colder than the SM, an observable yet *non-standard* $\Delta N_{\rm eff}$ effect can result from the non-thermal DR directly produced from DM annihilation. For IAnDM to yield detectable gravitational effects in the CMB and matter power spectrum (MPS), DM needs to be light and copious. In such mass range, MPS is dominantly affected by (*cold*) DM free-streaming. IAnDM with masses under ~ 200 keV is disfavored by current data, while future experiments will improve the sensitivity reach, especially if the late-time annihilation cross-section is enhanced relative to the standard thermal value, which can be generally realized (see discussion in Section. V).

II. An Example Model

The scenario of IAnDM can generally arise in particle physics models with thermal DM or beyond, while *our main results are largely model-independent*. We consider a simple example model where SM singlet fermionic DM χ annihilates into lighter fermionic DR particle ψ through a vector current interaction (Z' mediator), with s-wave thermal cross section, $\langle \sigma v \rangle$, which determines the relic abundance of χ, Ω_{χ}. The relevant Lagrangian is:

$$\mathcal{L} \supset i\bar{\chi}\slashed{D}\chi + i\bar{\psi}\slashed{D}\psi - m_{\chi}\bar{\chi}\chi - m_{\psi}\bar{\psi}\psi - \tfrac{1}{4}Z'_{\mu\nu}Z'^{\mu\nu} + \tfrac{1}{2}m_{Z'}^2 Z'^2,$$

where D_{μ} is the covariant derivative including Z' gauge interaction. The automatic self-scattering of χ or ψ mediated by a moderately massive Z' is generally ineffective at late times, so that ψ free-streams then (see [13] for an alternative case).

Without additional effective interactions, χ and ψ freeze out simultaneously as $\bar{\chi}\chi \to \bar{\psi}\psi$ departs from equilibrium. In this work we will assume that χ is the leading DM and thus the prediction for $\Omega_{\rm DM}$ resembles that of the standard WIMP DM. This requires ψ to be in form of dark radiation, much lighter than χ and freezes out while it is relativistic [50]. The temperature of a decoupled dark sector (χ, ψ) can be much colder than the SM, depending on the reheating pattern [17, 18] and the number of heavier states that have decoupled in each sector. The temperatures of χ, ψ also redshift differently after their freezeout. For the interest of this work, the relevant effect can be simply parametrized by $\xi \equiv \frac{\hat{T}_f}{T_f} \leq 1$ around the

dark thermal freezeout, where $\hat{T}_f$ is the dark temperature and T_f is the SM one.

Ω_χ can be estimated as in [5, 13]. We define freezeout temperature parameters $x_f \equiv \frac{m_\chi}{T_f}$, $\hat{x}_f \equiv \frac{m_\chi}{\hat{T}_f} = \frac{x_f}{\xi}$, and obtain

$$x_f \simeq \xi \ln \left(\sqrt{\frac{45}{16}} \frac{1}{\pi^3} \frac{g_\chi}{\sqrt{g_*}} m_\chi M_P \langle \sigma v \rangle \xi^{\frac{5}{2}} \right) \simeq \xi \hat{x}_f, \qquad (1)$$

$$\Omega_\chi^\infty = 0.32 \left(\frac{\hat{x}_f}{10} \right) \left(\frac{\sqrt{g_*}}{\sqrt{3.38}} \frac{43/11}{g_{*S}} \right) \left(\frac{3 \times 10^{-26} \text{ cm}^3 \text{ s}^{-1}}{\langle \sigma v \rangle / \xi} \right), \qquad (2)$$

where M_P is the Planck mass, g_χ is the internal degree of freedom (d.o.f) of χ, g_*, g_{*s} are the total effective d.o.f.'s dominated by SM states, and we use superscript ∞ to emphasize the IAnDM relic abundance is the asymptotic value (after some noticeable depletion, see Fig. 1). For a light sub-MeV DM, $\hat{x}_f \sim 10$, and around the DM freezeout $g_* = 3.38$, $g_{*s} = 43/11$ (the SM values after neutrino decoupling). Note that a fixed $\langle \sigma v \rangle / \xi \simeq \sigma_0 \equiv 3 \times 10^{-26}$ cm^3 s^{-1} is required to yield correct thermal DM abundance, therefore for $\xi < 1$, the required $\langle \sigma v \rangle$ is reduced by ξ accordingly. In order to make sure that ψ (hot relic) does not over close the Universe, we also check the thermal relic density of ψ:

$$\Omega_{\psi, \text{th}} = \begin{cases} \frac{m_\psi n_\psi}{\rho_c} = 0.038 \left(\frac{m_\psi}{1 \text{ eV}} \right) g_\psi \xi^3, & \text{massive } \psi; \\ 2.7 \times 10^{-4} g_\psi \xi^4, & \text{massless } \psi, \end{cases} \qquad (3)$$

where the subscript "th" denotes the thermal relic component of ψ, which distinguishes itself from the non-thermal component from χ annihilation that we will focus on (denoted by subscript "nth"). Note that for $\xi \ll 1$, $\Omega_{\psi, \text{th}}$ is strongly suppressed, even for a moderately massive ψ. $\xi < 1$ is also required by Big Bang nucleosynthesis [19] for sub-MeV DM.

III. Cosmological Effects of Invisible DM Annihilation: General Consideration and Analytic Studies

The non-thermal free-streaming DR ψ injected from DM χ annihilation contributes an additional radiation energy component to the Universe. Assuming $m_\psi = 0$ for simplicity, we can estimate the accumulated energy density of ψ from χ annihilation, $\rho_{\psi, \text{nth}}$, based on instantaneous energy conservation: $d\rho_{\psi, \text{nth}}(t) = \rho_\chi n_\chi \langle \sigma v \rangle dt$. Upon integration over time t' with proper redshift factors, the accumulated ψ density by the time t (a) is

$$\rho_{\psi, \text{nth}}(a) = \int_{a_i}^a \frac{\rho_{c,0}^2 \Omega_\chi^2}{m_\chi a'^6} \langle \sigma v \rangle \frac{a' da'}{H_0 \sqrt{\Omega_{\gamma + \nu}}} \left(\frac{a'}{a} \right)^4$$

$$= \left(\frac{3 H_0^2 \Omega_\chi}{8 \pi G} \right)^2 \frac{\langle \sigma v \rangle}{m_\chi H_0 \sqrt{\Omega_{\gamma + \nu}}} \frac{\ln(\frac{a}{a_i})}{a^4}. \qquad (4)$$

Here deep radiation dominated (RD) epoch is assumed, so Hubble parameter $H(a') \equiv da'/(a' dt') = H_0 \sqrt{\Omega_{\gamma + \nu}/a'^4}$ and $a_0 = 1$. a_i represents the initial time when the *net* ψ production from χ annihilation becomes effective which is around the freezeout time, $a/a_i \sim T_f/T$. Note that in addition to the standard redshift $1/a^4$, there is a moderate *log-dependence* on a which is different from either a fixed extra

neutrino background or many other non-cold DM-DR model, which is the key to the following characteristic signals.

In order to relate to the potential CMB observable, ΔN_{eff}, we take the ratio of $\rho_{\psi, \text{nth}}$ over SM neutrino density (one flavor), and find

$$\Delta N_{\text{eff, nth}}(a) = 0.038 \ln \left(\frac{a}{a_i} \right) \left(\frac{\text{keV}}{m_\chi/\xi} \right) \left(\frac{\langle \sigma v \rangle / \xi}{3 \times 10^{-26} \text{ cm}^3/\text{s}} \right), \qquad (5)$$

where $a \approx 10^{-3}$ when evaluated around the CMB epoch. Note that $\Delta N_{\text{eff, nth}}$ inherits the aforementioned $\ln (a/a_i)$ dependence. Apparently lighter DM produce more copious ψ and thus more pronounced signals. We can also see that with $\xi = 1$ and thus $\langle \sigma v \rangle = \sigma_0$, an $O(1) - O(10)$ keV mass χ could lead to an observable ΔN_{eff} at current or upcoming CMB experiments [20–22], while for $\xi < 1$ and fixed $\langle \sigma v \rangle / \xi \equiv \sigma_0$ a lighter χ is required to yield the same ΔN_{eff}. Therefore we will parametrize with *the rescaled DM mass, m_χ/ξ* in Figures.

Fig. 1 illustrates the physics discussed above. In the upper panel, the deviation of DM's co-moving density, $Y_\chi(a)$, from its current-day value, is calculated by numerically solving the Boltzmann equation around DM freezeout. In the lower panel, along with the novel residual annihilation induced $\Delta N_{\text{eff, nth}}$, the irreducible thermal contribution to ΔN_{eff} is also shown (relevant if $m_\psi \lesssim$ eV):

$$\Delta N_{\text{eff, th}} = 3.046 \frac{\rho_{\psi, \text{th}}}{\rho_{\nu, 1}} = 2.2 g_\psi \xi^4, \qquad (6)$$

where $\rho_{\nu, 1}$ is the energy density of 1 generation of SM neutrino. We can see that $\Delta N_{\text{eff, nth}}$ can easily dominates over $\Delta N_{\text{eff, th}}$.

IAnDM model may also affect MPS in various ways. For the parameter range that leads to observable effects (light χ), the dominating factor is the free-streaming of χ following its freezeout. Although IAnDM freezes out as a cold relic, with sufficiently small mass (e.g. $O(100)$ keV), it decouples late enough to sustain a non-negligible free-streaming effect for LSS (also see [23]). As shown in the later Fig. 3, at leading order the MPS from IAnDM resembles that due to a thermal WDM model with a corresponding m_{WDM}, which shows suppression at a much larger scale (kpc to Mpc) compared to a typical WIMP clump (pc) [24, 25], thus is subject to current Lyman-α constraints. The $\chi - \psi$ scattering may induce a competing suppression through dark acoustic oscillation [24, 25], but we have checked that with a massive Z' and $\xi < 1$ the $\chi - \psi$ kinetic decoupling occurs early enough and does not affect MPS effectively [51]. A correspondence between IAnDM and WDM can be derived analytically by matching the free-streaming velocity, $v_{\text{FS}}(a)$, in the two models, which plays an important role in perturbation Boltzmann equations [26] (this is similar to the correspondence between the sterile neutrino case and thermal WDM [27]). In non-relativistic limit, $v_{\text{FS}}(a) = \frac{p}{E} \rightarrow \frac{\tilde{p}}{m} \frac{1}{a}$, where $\tilde{}$ denotes co-moving quantities. Therefore if the v_{FS}'s match today $(a = 1)$, they also match at earlier times relevant to structure formation. Taking into
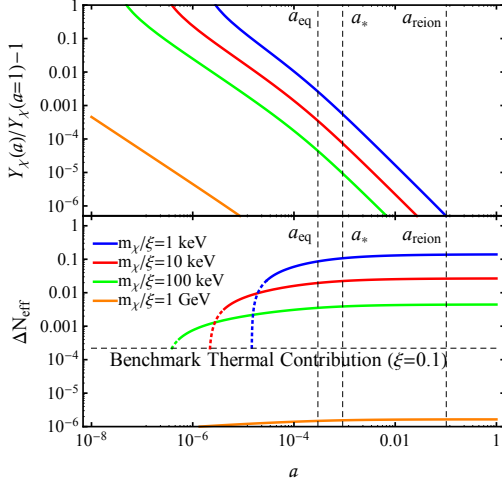
FIG. 1: Upper panel: the slow depletion of Y_χ due to its residual annihilation. Lower panel: $\Delta N_{\rm eff}$ due to massless annihilation product ψ. $a_{\rm eq}$, a_*, $a_{\rm reion}$ are the expansion parameters, at the matter-radiation equality, recombination and reionization epochs, respectively. Here we include proper redshift for both RD and matter-dominated (MD) eras.

account the specifics around freezeout in IAnDM and WDM models, we find that at $a = 1$: $\tilde{p}_{\rm WDM} = \left(\frac{2\pi^2}{3\zeta(3)}\frac{\rho_{\rm WDM}}{m_{\rm WDM}}\right)^{\frac{1}{3}}$, $\tilde{p}_\chi = \sqrt{3\hat{x}_f}\xi T_\gamma$, where T_γ is $T_{\rm CMB}$ today. Equating $\frac{\tilde{p}}{m}$ in the two models, we find the correspondence:

$$m_{\rm WDM} = \left(\frac{2\pi^2\rho_{\rm WDM}}{3\zeta(3)}\right)^{\frac{1}{4}}\left(\frac{m_\chi/\xi}{T_\gamma\sqrt{3\hat{x}_f}}\right)^{\frac{3}{4}} = 0.07\left(\frac{m_\chi/\xi}{\rm keV}\right)^{\frac{3}{4}} {\rm keV},$$
(7)

where we took $\rho_{\rm WDM} = \rho_{\rm DM,0}$, $\hat{x}_f = 10$.

IV. Numerical Studies

We further perform a numerical analysis by solving the perturbation Boltzmann equations for the evolution of the χ, ψ system using camb [28]. The general formulation follows [26] with the choice of synchronous gauge. The dominant DM, χ, follows the standard treatment while allowing DM free-streaming effect. As Ω_χ will slowly decrease due to annihilation, for fixed $\langle\sigma v\rangle$ we numerically iterate to align it with the CDM value at matter radiation equality. The initial perturbation of the annihilation product, ψ, inherits that of χ (CDM), while its later evolution follows the same perturbation multipole expansion as the massless or massive neutrinos. Therefore for the partition function of both χ and ψ, $f = f(\tilde{p})(1 + \Psi) = f(\tilde{p})(1 + \Psi(\tau, x^i, p, n_i))$, i.e., the unperturbed $f(\tilde{p})$ is corrected by small fractional perturbation Ψ.

The perturbative Boltzmann equation for multipole ℓ is

$$\partial_\tau\Psi_0 = -\frac{\tilde{p}}{\tilde{E}}k\Psi_1 + \frac{1}{6}\partial_\tau h\frac{d\ln f(\tilde{p})}{d\ln\tilde{p}},$$
(8)

$$\partial_\tau\Psi_1 = \frac{\tilde{p}}{\tilde{E}}k\left(\Psi_0 - \frac{2}{3}\Psi_2\right),$$
(9)

$$\partial_\tau\Psi_2 = \frac{\tilde{p}}{\tilde{E}}k\left(\frac{2}{5}\Psi_1 - \frac{3}{5}\Psi_3\right)$$
(10)

$$- \left(\frac{1}{15}\partial_\tau h + \frac{2}{5}\partial_\tau\eta\right)\frac{d\ln f(\tilde{p})}{d\ln\tilde{p}},$$
(11)

$$\partial_\tau\Psi_\ell = \frac{\tilde{p}}{\tilde{E}}\frac{k}{2\ell+1}\left(\ell\Psi_{\ell-1} - (\ell+1)\Psi_{\ell+1}\right)\quad \ell \geq 3,$$
(12)

$$\partial_\tau\Psi_\ell = \frac{\tilde{p}}{\tilde{E}}k\Psi_{\ell-1} + \frac{\ell+1}{\tau}\Psi_\ell \qquad {\rm As\ Truncation.}$$
(13)

Here we choose the synchronous gauge $g_{\mu\nu} = a^2(^{-1}{}_{\delta_{ij}+h_{ij}})$, and $h_{ij}(\vec{x}) = \int\frac{d^3k}{(2\pi)^{3/2}}e^{i\vec{k}\cdot\vec{x}}\left(\hat{k}_i\hat{k}_jh(\vec{k}) + (\hat{k}_i\hat{k}_j - \frac{1}{3}\delta_{ij})6\eta(\vec{k})\right)$, which gives the definition of metric perturbation of h and η.

However there are key differences between neutrinos and the ψ produced from DM annihilation. First, unlike neutrinos, the unperturbed partition function $f(\tilde{p})$ of ψ is not thermal, rather it is given by the annihilation process with a fixed physical momentum (determined by m_χ, m_ψ). The $f(\tilde{p})$ feeds into the perturbation equations through the factor of $\frac{\partial\ln f(\tilde{p})}{\partial\ln\tilde{p}}$, which can be replaced by -4 for massless neutrinos. For our non-thermally produced ψ, this factor can be calculated in the same way as in [29], which at leading order yields: $\frac{\partial\ln f(\tilde{p})}{\partial\ln\tilde{p}} = -\frac{9}{2} + \frac{3\bar{p}}{2\bar{\rho}}$, where $\bar{p}, \bar{\rho}$ are the background pressure and energy density. Numerically we also include a small $\mathcal{O}(\frac{\Gamma_{\rm ann}}{H})$ correction to this factor. Moreover, the binning of ψ in the comoving momentum space is different from that of neutrino: for a fixed a only the modes with $\tilde{p} < a\sqrt{m_\chi^2 - m_\psi^2}$ contribute. We choose the standard cosmology parameters: $h = 0.678$, $\Omega_\chi h^2 \approx \Omega_{\rm DM}h^2 = 0.1186$, $\Omega_b h^2 = 0.02226$, etc. [21]

Numerical Results: The CMB Signatures

In Fig. 2 we plot the zoomed-in CMB TT spectra around the first and the sixth acoustic peaks, for a set of m_χ/ξ choices, in comparison with CDM and standard $\Delta N_{\rm eff}$ models. As expected based on our analytic estimate (Eq. 5), the effects from ψ injection at leading order resemble that from standard $\Delta N_{\rm eff}$, which as shown below are confirmed by numerical studies. However, as we will explain, there are key differences between a genuine $\Delta N_{\rm eff}$ and the $\Delta N_{\rm eff}$-like effect caused by non-thermal ψ.

The most notable effect on the CMB spectrum due to $\Delta N_{\rm eff}$ or non-thermal ψ in IAnDM is on the heights of the acoustic peaks. In both models, the change to H due to additional radiation energy density leads to the increase in the height of the first peak (i.e., early integrated Sachs-Wolfe (ISW) effect), and the decrease in that of the higher peaks (i.e., enhanced Silk damping). However, the heights of CMB acoustic peaks from
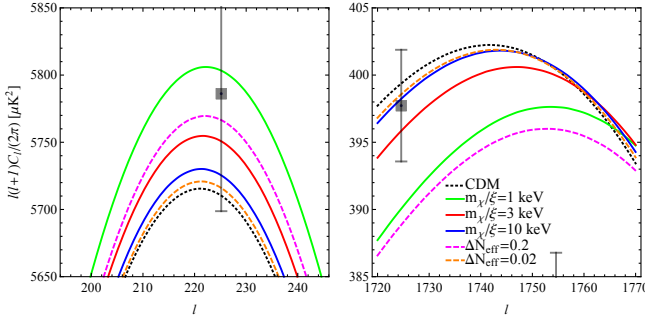
FIG. 2: An illustration of CMB signals of IAnDM with fixed cosmological parameters (see text). Also shown are the spectra with CDM and $\Delta N_{\rm eff} = 0.02,\ 0.2$ for comparison, as well as the binned error bars of Planck data. Left panel: TT mode around the first acoustic peak; right panel: around the sixth acoustic peak. Note that this should not be used to extract phase shift since θ_*, θ_D and $z_{\rm eq}$ are not fitted to observations.

IAnDM do not align with those due to a fixed standard $\Delta N_{\rm eff}$. As expected (Eq. 5 and Fig. 1), $\Delta N_{\rm eff,nth}$ varies over time as $\rho_{\psi,\rm nth}$ accumulates while χ continues to annihilate. This can be seen by comparing the amplitudes of the CMB spectrum shown in Fig. 2 where higher ℓ corresponds to an earlier time (when the mode re-enters horizon): consider a fixed $m_\chi/\xi = 1$ keV, around the 6th peak the resulting CMB TT spectrum roughly aligns with that associated with $\Delta N_{\rm eff} \approx 0.12$; while around the 1st peak, it aligns with a larger $\Delta N_{\rm eff} \approx 0.35$.

The standard $\Delta N_{\rm eff}$ also reveals itself via a unique phase shift of the high ℓ acoustic peaks due to neutrino-like modes that induce a significant anisotropic stress and propagate faster than the sound speed (free-streaming) [30, 31], which cannot be caused by other standard physics [52]. IAnDM induces a phase shift as well, yet with dramatic difference compared to that caused by standard $\Delta N_{\rm eff}$. We found that by adjusting h, $\Omega_{\rm DM}h^2$, $Y_{\rm He}$ to match the CMB observables of θ_*, θ_D and $z_{\rm eq}$ [21], in the IAnDM model the locations of the acoustic peaks shift towards high ℓ's, *opposite* to the direction expected from standard free-streaming $\Delta N_{\rm eff}$ [30]. Such an effect resembles that due to fluid-like DR species [13, 31, 32], yet for different reasons. Even though free-streaming, unlike neutrinos, the non-thermal ψ dominantly produced at late times *inherits a negligible initial anisotropic stress from χ*, and consequently would not induce an additional phase shift along the same direction as neutrinos [53]. However, such ψ does contribute to late-time radiation energy density, and thus reduce the energy fraction of the free-streaming SM neutrinos. As noted in [13] such a reduction (due to fluid-like DR or non-thermal ψ here) leads to a phase shift along the direction opposite to that due to standard $\Delta N_{\rm eff}$. Furthermore, just as with peak heights, there is scale dependence in phase shifts, which is a higher order effect that may distinguish IAnDM from fluid-like DR (see [33] for a related recent work) [54].

Numerical Results: The Matter Power Spectra

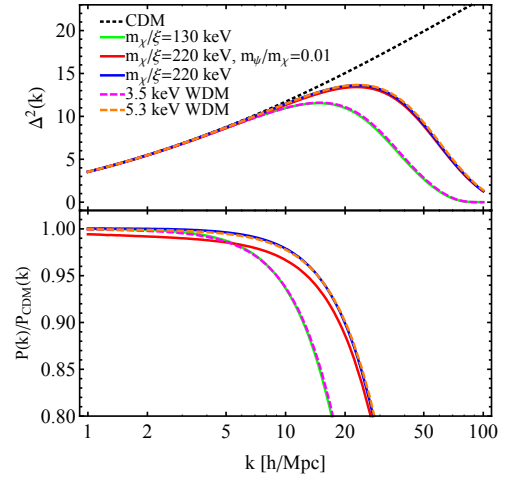In Fig. 3 we present the MPS in the scenario of IAnDM, in comparison with other familiar new physics scenario: CDM

FIG. 3: Matter power spectra for different DM χ masses and different m_ψ/m_χ and $\langle\sigma v\rangle$ ($m_\psi = 0$, with one exception). Also shown are the 3.5 keV, 5.3 keV WDM spectra (saturating the current conservative and aggressive Lyman-α bound [35]) .
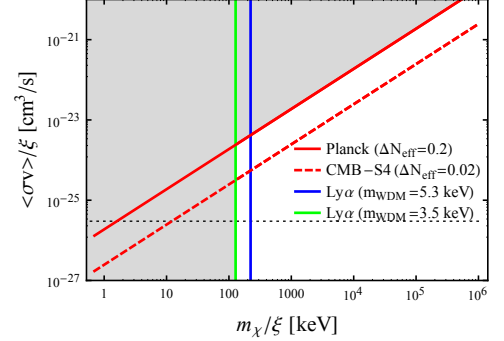

FIG. 4: The (projected) constraints on IAnDM from Planck and CMB-S4 (for details see text), and from Lyman-α measurements ($m_\psi = 0$, fixed $\langle\sigma v\rangle$), shaded region is excluded. We assume all DM to be χ, but allow mechanisms other than thermal freeze-out for its production. The axes are labeled by taking into account the rescaling factor $\xi = T_{\rm DM}/T_{\rm SM}$ at freezeout time. Dashed line is a reference to standard thermal freezeout cross-section.

and WDM. Compared to the standard CDM prediction, all these new models cause a suppression of MPS relative to the standard cosmology for $k \gtrsim 1\ h/{\rm Mpc}$. The upper panel $\Delta^2(k) = \frac{k^3}{2\pi^2}P(k)$ [34] shows that the IAnDM spectra well overlaps with WDM spectra with a corresponding mass estimated by Eq. 7. Nevertheless, the zoomed-in bottom panel of Fig. 3 shows slight differences between IAnDM and WDM spectra, allowing a massive ψ (still require $m_\psi \ll m_\chi$ to be consistent with our starting assumption on cosmology). The suppression on small scales is more pronounced for a massive ψ, which can be understood as a massive ψ contributes more energy density at the structure formation time than a massless ψ, boosting the free streaming effect.

V. Summary and Discussion

With our understanding of the IAnDM effects on the CMB

and the MPS, we can derive constraints based on current data and project sensitivities for future experiments. The results are summarized in Fig. 4, where we label the axes with the scaling factor ξ to account for the generic colder dark sector possibility. The CMB constraint is calculated by Fisher forecast, which agrees well with the estimate by comparing the (projected) experimental sensitivity limit on $\Delta N_{\rm eff}$ and our analytical formula Eq. 5. On the other hand, the MPS constraint is extracted by comparing the DM free-streaming effect based on our Eq. 7. Note that the main effect of IAnDM on the CMB depends on the ratio $\langle \sigma v \rangle / m_\chi$ (Eq. 5). The current Planck (projected CMB-S4) sensitivity for fixed $\Delta N_{\rm eff}$, $\sigma_{N_{\rm eff}} \simeq 0.2$ [21, 32] ($\sigma_{N_{\rm eff}} \simeq 0.02$ [22, 36–38]), gives a bound of $m_\chi/\xi \gtrsim 1.6$ keV ($m_\chi/\xi \gtrsim 12$ keV), assuming standard thermal $\langle \sigma v \rangle / \xi$. In contrast, the main effect of IAnDM on MPS only depends on m_χ/ξ (Eq. 7), insensitive to $\langle \sigma v \rangle$. The current Lyman-α observation constrains IAnDM MPS: the 2σ aggressive bound ($m \gtrsim 5.3$ keV for WDM) corresponds to a bound of $m_\chi/\xi \gtrsim 220$ keV, and the conservative bound ($m \gtrsim 3.5$ keV for WDM) corresponds to a bound of $m_\chi/\xi \gtrsim 130$ keV.

Note that although in this work we considered a particular thermal IAnDM model as a simple example, the inferred novel phenomenology applies to broader possibilities of IAnDM models allowing an enhanced annihilation cross-section relative to the standard thermal value. Such possibilities have been well considered in the context of the familiar visibly annihilating DM, including: Sommerfeld enhancement [39–41] (automatic in IAnDM if DR is a light mediator instead of a fermion), enhancement due to non-standard cosmology or non-thermal production of DM [42–44].

Astrophysical/cosmological observation is stepping into a high precision era, which enables us to probe well-motivated DM models that are beyond the reach of conventional DM detections. In this *Letter* we demonstrate a representative example by investigating the novel phenomenology from the minimal and generic scenario of Invisibly Annihilating DM (IAnDM). The smoking gun signature of this large class of models includes a correlated combination of scale-dependent, fluid-like $\Delta N_{\rm eff}$ in the CMB spectra and a characteristic matter power spectrum that resembles WDM. The current data constrains the IAnDM with masses up to ~ 200 keV, while future experiments can be sensitive to larger masses if the DM annihilation cross-section is enhanced relative to the standard thermal value. These findings motivate new dedicated analyses to optimize the potential for discovering DM residing in a hidden sector.

* Electronic address: yanou.cui@ucr.edu
† Electronic address: huora@ucr.edu

[1] N. Padmanabhan and D. P. Finkbeiner, Phys. Rev. **D72**, 023508 (2005), astro-ph/0503486.
[2] M. S. Madhavacheril, N. Sehgal, and T. R. Slatyer, Phys. Rev. **D89**, 103508 (2014), 1310.3815.
[3] D. Green, P. D. Meerburg, and J. Meyers (2018), 1804.01055.
[4] M. Pospelov, A. Ritz, and M. B. Voloshin, Phys. Lett. **B662**, 53 (2008), 0711.4866.
[5] J. L. Feng, H. Tu, and H.-B. Yu, JCAP **0810**, 043 (2008), 0808.2318.
[6] C. Cheung, G. Elor, L. J. Hall, and P. Kumar, JHEP **03**, 085 (2011), 1010.0024.
[7] J. M. Cline and A. R. Frey, Phys. Lett. **B706**, 384 (2012), 1109.4639.
[8] G. Belanger and J.-C. Park, JCAP **1203**, 038 (2012), 1112.4491.
[9] M. Blennow, E. Fernandez-Martinez, O. Mena, J. Redondo, and P. Serra, JCAP **1207**, 022 (2012), 1203.5803.
[10] C. Garcia-Cely, A. Ibarra, and E. Molinaro, JCAP **1402**, 032 (2014), 1312.3578.
[11] K. Agashe, Y. Cui, L. Necib, and J. Thaler, JCAP **1410**, 062 (2014), 1405.7370.
[12] J. Berger, Y. Cui, and Y. Zhao, JCAP **1502**, 005 (2015), 1410.2246.
[13] Z. Chacko, Y. Cui, S. Hong, and T. Okui, Phys. Rev. **D92**, 055033 (2015), 1505.04192.
[14] Z. Chacko, Y. Cui, S. Hong, T. Okui, and Y. Tsai, JHEP **12**, 108 (2016), 1609.03569.
[15] M. H. Chan, Astropart. Phys. **80**, 1 (2016), 1604.01494.
[16] T. Bringmann, F. Kahlhoefer, K. Schmidt-Hoberg, and P. Walia, Phys. Rev. **D98**, 023543 (2018), 1803.03644.
[17] Z. G. Berezhiani, A. D. Dolgov, and R. N. Mohapatra, Phys. Lett. **B375**, 26 (1996), hep-ph/9511221.
[18] P. Adshead, Y. Cui, and J. Shelton, JHEP **06**, 016 (2016), 1604.02458.
[19] R. H. Cyburt, B. D. Fields, K. A. Olive, and T.-H. Yeh, Rev. Mod. Phys. **88**, 015004 (2016), 1505.01076.
[20] A. Suzuki et al. (POLARBEAR), J. Low. Temp. Phys. **184**, 805 (2016), 1512.07299.
[21] P. A. R. Ade et al. (Planck) (2015), 1502.01589.
[22] K. N. Abazajian et al. (CMB-S4) (2016), 1610.02743.
[23] S. Das and K. Sigurdson, Phys. Rev. **D85**, 063510 (2012), 1012.4458.
[24] A. Loeb and M. Zaldarriaga, Phys. Rev. **D71**, 103520 (2005), astro-ph/0504112.
[25] E. Bertschinger, Phys. Rev. **D74**, 063509 (2006), astro-ph/0607319.
[26] C.-P. Ma and E. Bertschinger, Astrophys. J. **455**, 7 (1995), astro-ph/9506072.
[27] M. Viel, J. Lesgourgues, M. G. Haehnelt, S. Matarrese, and A. Riotto, Phys. Rev. **D71**, 063534 (2005), astro-ph/0501562.
[28] A. Lewis, A. Challinor, and A. Lasenby, Astrophys. J. **538**, 473 (2000), astro-ph/9911177.
[29] R. Huo, Phys. Lett. **B701**, 530 (2011), 1104.4094.
[30] S. Bashinsky and U. Seljak, Phys. Rev. **D69**, 083002 (2004), astro-ph/0310198.
[31] D. Baumann, D. Green, J. Meyers, and B. Wallisch, JCAP **1601**, 007 (2016), 1508.06342.
[32] C. Brust, Y. Cui, and K. Sigurdson, JCAP **1708**, 020 (2017), 1703.10732.

[33] G. Choi, C.-T. Chiang, and M. LoVerde (2018), 1804.10180.

[34] S. Dodelson, *Modern Cosmology* (Academic Press, Amsterdam, 2003), ISBN 9780122191411.

[35] V. Irsic et al., Phys. Rev. **D96**, 023522 (2017), 1702.01764.

[36] W. L. K. Wu, J. Errard, C. Dvorkin, C. L. Kuo, A. T. Lee, P. McDonald, A. Slosar, and O. Zahn, Astrophys. J. **788**, 138 (2014), 1402.4108.

[37] J. Errard, S. M. Feeney, H. V. Peiris, and A. H. Jaffe (2015), 1509.06770.

[38] K. N. Abazajian et al. (Topical Conveners: K.N. Abazajian, J.E. Carlstrom, A.T. Lee), Astropart. Phys. **63**, 66 (2015), 1309.5383.

[39] N. Arkani-Hamed, D. P. Finkbeiner, T. R. Slatyer, and N. Weiner, Phys. Rev. **D79**, 015014 (2009), 0810.0713.

[40] J. L. Feng, M. Kaplinghat, and H.-B. Yu, Phys. Rev. **D82**, 083525 (2010), 1005.4678.

[41] T. Binder, M. Gustafsson, A. Kamada, S. M. R. Sandner, and M. Wiesner (2017), 1712.01246.

[42] G. B. Gelmini and P. Gondolo, Phys. Rev. **D74**, 023510 (2006), hep-ph/0602230.

[43] J. Fan, O. zsoy, and S. Watson, Phys. Rev. **D90**, 043536 (2014), 1405.7373.

[44] A. L. Erickcek, Phys. Rev. **D92**, 103505 (2015), 1504.03335.

[45] M. Farina, D. Pappadopulo, J. T. Ruderman, and G. Trevisan, JHEP **12**, 039 (2016), 1607.03108.

[46] R. Huo, M. Kaplinghat, Z. Pan, and H.-B. Yu (2017), 1709.09717.

[47] B. Follin, L. Knox, M. Millea, and Z. Pan, Phys. Rev. Lett. **115**, 091301 (2015), 1503.07863.

[48] B. Audren, J. Lesgourgues, G. Mangano, P. D. Serpico, and T. Tram, JCAP **1412**, 028 (2014), 1407.2418.

[49] V. Poulin, P. D. Serpico, and J. Lesgourgues, JCAP **1608**, 036 (2016), 1606.02073.

[50] If ψ is massive enough, its relic density today can dominate over that of χ [45], which is an interesting alternative scenario that we will leave for future investigation.

[51] For example with $\xi = 0.1$, $m_\chi = 1$ keV and $g_\chi = 0.5$, the $m_{Z'}$ to reproduce thermal freezeout $\langle \sigma v \rangle / \xi$ is 80 MeV, and kinetic decoupling $T_{\rm kd} = 2.4$ keV from Eq. 2 of [46] happens earlier than chemical freezeout $T_f = 1$ keV. This is due to a much colder dark sector, where the DR ψ number density is ξ^3 suppressed. Therefore in our numerical calculation we have ignored the $\chi - \psi$ scattering.

[52] Such an effect from SM neutrinos was recently detected with Planck data [47].

[53] Although ψ may develop a larger anisotropic stress after production, our numerical analysis shows that its effect on CMB phase shift is subdominant to what we discussed in this paper.

[54] Qualitatively the novel effects on CMB anisotropy spectrum we discussed here may also originate from the scenario of DM decaying to DR [29, 48, 49]. However, for decaying DM with long enough lifetime to be cosmologically stable and satisfy existing constraints, the amount of DR produced during CMB epoch is tiny and the resultant signal strength is expected to be negligible.